JCI insight

RESEARCH ARTICLE

IFN-ε protects primary macrophages against HIV infection

Carley Tasker,[1] Selvakumar Subbian,[2] Pan Gao,[3] Jennifer Couret,[1] Carly Levine,[2] Saleena Ghanny,[1] Patricia Soteropoulos,[1] Xilin Zhao,[1,2] Nathaniel Landau,[4] Wuyuan Lu,[3] and Theresa L. Chang[1,2]

[1]Department of Microbiology, Biochemistry and Molecular Genetics and [2]Public Health Research Institute, Rutgers University, New Jersey Medical School, Newark, New Jersey, USA.[3]Institute of Human Virology, University of Maryland School of Medicine, Baltimore, Maryland, USA.[4]Department of Microbiology, New York University School of Medicine, New York, New York, USA.

IFN-ε is a unique type I IFN that is not induced by pattern recognition response elements. IFN-ε is constitutively expressed in mucosal tissues, including the female genital mucosa. Although the direct antiviral activity of IFN-ε was thought to be weak compared with IFN-α, IFN-ε controls *Chlamydia muridarum* and herpes simplex virus 2 in mice, possibly through modulation of immune response. We show here that IFN-ε induces an antiviral state in human macrophages that blocks HIV-1 replication. IFN-ε had little or no protective effect in activated CD4⁺ T cells or transformed cell lines unless activated CD4⁺ T cells were infected with replication-competent HIV-1 at a low MOI. The block to HIV infection of macrophages was maximal after 24 hours of treatment and was reversible. IFN-ε acted on early stages of the HIV life cycle, including viral entry, reverse transcription, and nuclear import. The protection did not appear to operate through known type I IFN-induced HIV host restriction factors, such as APOBEC3A and SAMHD1. IFN-ε–stimulated immune mediators and pathways had the signature of type I IFNs but were distinct from IFN-α in macrophages. IFN-ε induced significant phagocytosis and ROS, which contributed to the block to HIV replication. These findings indicate that IFN-ε induces an antiviral state in macrophages that is mediated by different factors than those induced by IFN-α. Understanding the mechanism of IFN-ε–mediated HIV inhibition through immune modulation has implications for prevention.

Introduction

Type I IFNs play a key role in immune responses and control of cell growth (1). In humans, 13 IFN-α subtypes and one each of IFN-β, IFN-ε, IFN-κ, and IFN-ω comprise the type I IFNs (2). IFN-α/β have been studied extensively, but the functions of other members are less understood. Basal levels of IFN-α/β are low or undetectable, but their expression can be induced rapidly and significantly in response to infection (1, 3). IFN-α/β are important for controlling viral replication and priming adaptive responses during acute infection (4–9). However, unregulated type I IFN responses have been associated with progression of viral infections, including HIV (10–15). A complex role of type I IFNs in HIV infection has been well documented (15–20). A recent study in rhesus macaques with SIV infection showed that blocking IFN-I receptor function resulted in an increase in viral load during acute infection and disease progression; paradoxically, administration of IFN-α2 produced a similar outcome, resulting in greater CD4⁺ T cell depletion and faster disease progression, despite initial control of the viral infection (11).

Human IFN-ε is encoded on chromosome 9p21 (chromosome 4 in mice), along with the other type I IFNs. In mice, IFN-ε induces IFN-regulated genes, including *Irf-7* and *2'5'oas*, through Ifnar1 or Ifnar2 (21, 22). IFN-ε shares 30% amino acid homology with a consensus IFN-α and IFN-β sequence (22); however, IFN-ε displays distinct functions compared with IFN-α (22, 23). Unlike IFN-α, IFN-ε gene expression is not induced in response to activation of pattern recognition receptor pathways, such as TLRs 2, 3, 4, 7/8, and 9 (21). Forced expression of IRF3, IRF5, or IRF7 induces the promoter activity of IFN-α/β but not of IFN-ε (21). Unlike IFN-α/β, expression of IFN-ε is not induced in response to infection by viruses, including Semliki Forest virus, herpes simplex virus 2, mengovirus, and SIV, or by bacteria, such *Chlamydia*, in vitro or in mice (21, 24, 25). Although the antiviral activity of IFN-ε is much weaker than that of IFN-α (26, 27), IFN-ε–null mice are more susceptible to herpes simplex virus 2 infection (21). Forced expression

Conflict of interest: The authors have declared that no conflict of interest exists.

Submitted: April 28, 2016
Accepted: October 27, 2016
Published: December 8, 2016

Reference information:
JCI Insight. 2016;1(20):e88255.
doi:10.1172/jci.insight.88255.

of IFN-ε (via a vaccinia vector) induces rapid viral clearance in the lung (23). The antiviral activity was associated with recruitment of increased numbers of lymphocytes and elevated cytotoxic T cell subsets in lung (23). The nonsense nucleotide polymorphism in IFN-ε has been associated with increased risks to develop vitiligo or intracerebral hemorrhage (28, 29), possibly through immune dysregulation, suggesting its role in immune-associated diseases in humans.

In contrast to IFN-α/β, IFN-ε is constitutively expressed in various mucosal tissues, including lung, small intestine, and reproductive tissues (21, 22). IFN-ε is highly expressed in the female reproductive tract and appears to be induced by estrogen in mice (21). Additionally, TNF-α induces IFN-ε but not IFN-α/β in HeLa cells (30). IFN-ε induction has been reported in cervical tissues in response to seminal plasma (31). Interestingly, HIV-negative sex workers with frequent exposure to semen have an increased level of IFN-ε gene expression in the cervical epithelium (32). Taken together, IFN-ε plays a role distinct from type I IFNs in mucosal immunity against pathogens.

Here, we examined effects and underlying mechanisms of IFN-ε in HIV infection of monocyte-derived macrophages (MDMs). We found that IFN-ε blocked HIV replication in macrophages. It acted on early stages of the HIV life cycle, including entry, reverse transcription, and nuclear import. It did not appear to operate through known IFN-induced HIV host restriction factors. IFN-ε induced immune responses in primary macrophages distinct from those induced by IFN-α. Importantly, we discovered a protective effect of IFN-ε in primary macrophages against HIV by surging ROS.

Results

IFN-ε blocks HIV-1 infection of primary macrophages. We first determined the effect of IFN-ε on HIV-1 infection of primary macrophages, activated $CD4^+$ T cells, and cell lines that are susceptible to HIV infection. MDMs were treated with different concentrations of IFN-ε for 24 hours before exposure to HIV-1 primary isolates (Figure 1A). These included early transmitted/founder (T/F) viruses isolated during acute infection that have distinct features from those isolated in chronic infection (33). In addition, a single-cycle HIV-1 luciferase reporter virus pseudotyped with CCR5 using (R5) HIV envelope JR-FL, HIV-luc (JR-FL), was used (Figure 1B). After removal of unbound virus, infected cells were cultured in the absence of IFN-ε, and HIV infection was determined by measuring HIV p24 in the media (Figure 1A) or luciferase activity (Figure 1B). Treatment of MDMs with IFN-ε for 24 hours blocked replication of R5, X4, and dual-tropic X4R5 primary isolates (Figure 1A). IFN-ε also protected macrophages from infection by T/F viruses (Figure 1A). IFN-ε reduced the single-cycle infection of MDMs from multiple donors by 70%–98% (Figure 1B).

IFN-ε protected MDMs against HIV infection regardless of the source of IFN-ε, including yeast, mammalian cells (Expi293F), or bacteria, although bacteria-expressed IFN-ε was somewhat less potent (Figure 1C). Human IFN-ε has three Cys residues. Linearization of IFN-ε by reduction/alkylation abrogated its anti-HIV activity (Figure 1C). MDMs are highly sensitive to the inhibition of HIV infection by LPS. LPS was not detected in the IFN-ε stock; however, to rule out the possibility that the inhibitory effect was caused by trace LPS contamination, we added polymyxin B (PmB) to the cultures and found that PmB abolished LPS-mediated HIV inhibition but not the effect of IFN-ε (Supplemental Figure 1A; supplemental material available online with this article; doi:10.1172/jci.insight.88255DS1). Additionally, anti-HIV activity of IFN-ε was not due to cytotoxicity (Supplemental Figure 1B).

We next tested the effect of IFN-ε on HIV infection of PHA-activated $CD4^+$ T cells, HeLa-CD4-CCR5 cells, or PMA-treated THP-1 cells (macrophage phenotype). We found that IFN-ε did not protect activated $CD4^+$ T cells (Figure 1D) or HeLa-CD4-CCR5 cells (Supplemental Figure 2) in a single-cycle infection assay. IFN-ε strongly reduced viral replication of $CD4^+$ T cells infected by $HIV\text{-}1_{BaL}$ at a low MOI (0.01) but not at a higher MOI (0.05), the titer for infecting MDMs (Figure 1D). Unlike IFN-ε, IFN-α (IFNα 2 subtype) blocked HIV replication in $CD4^+$ T cells at both MOIs (Figure 1D). We then determined anti-HIV activity of IFN-ε using two THP-1 cell lines (line 1 and line 2) originally obtained from ATCC but maintained in two different laboratories. IFN-ε had a slight ability to either promote (line 1) or inhibit (line 2) HIV infection of PMA-treated THP-1 cells, whereas IFN-α efficiently blocked infection (Figure 1E), suggesting that pathways involved in the inhibitory activity of these two IFNs are not identical. SAMHD1 is a myeloid cell restriction factor that is induced in specific cell types by type I IFNs (34, 35). To determine whether SAMHD1 plays a role in the IFN-ε antiviral activity, we assessed the effect of IFN-ε on HIV infection of THP-1 with an shRNA stable knockdown of SAMHD1 (36). Consistent with previous reports, the degree of HIV infection increased in the SAMHD1 knockdown cells. IFN-α blocked HIV infection in the

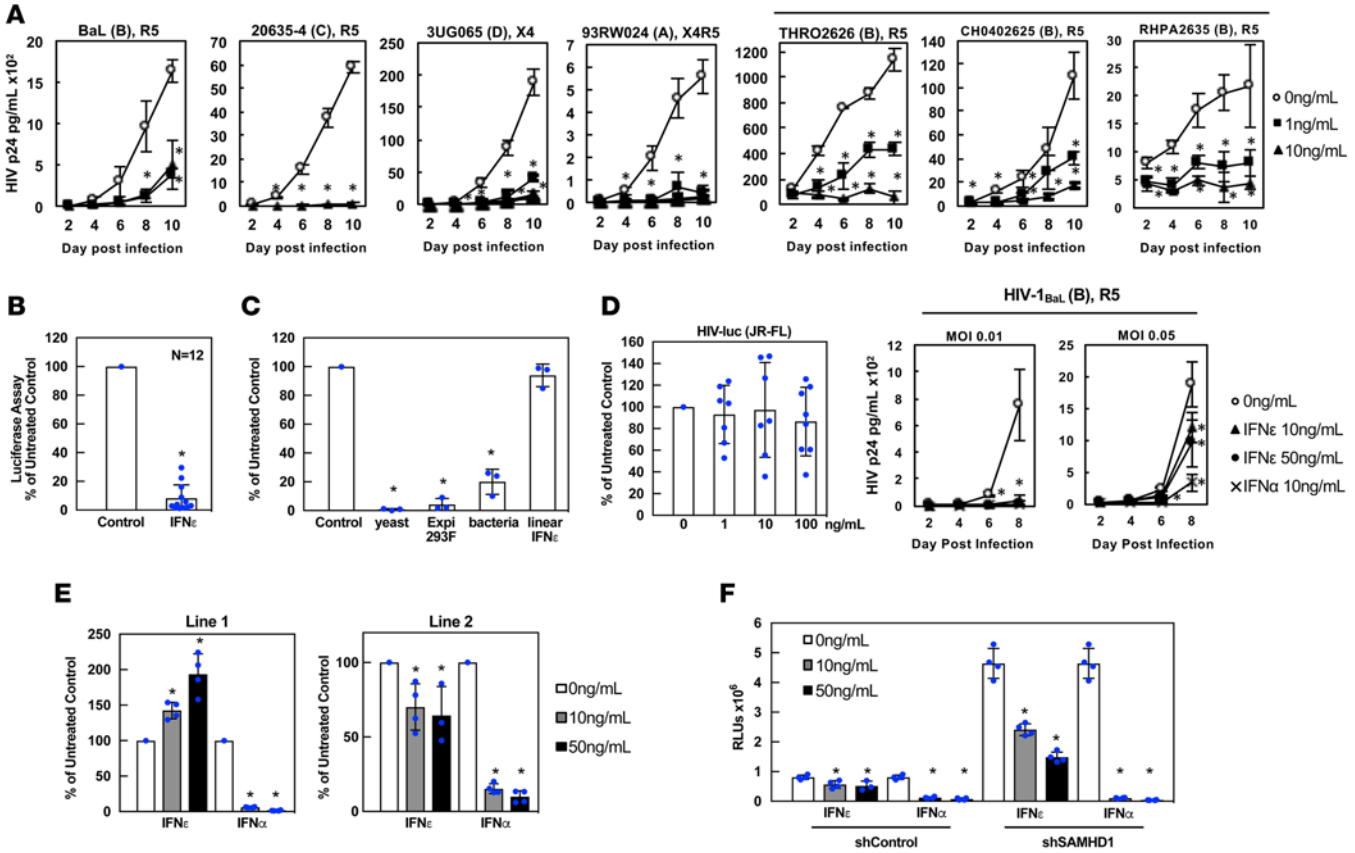

Figure 1. IFN-ε protects primary macrophages from HIV infection. (**A**) IFN-ε inhibits HIV replication. MDMs were treated with IFN-ε for 24 hours and then exposed to HIV-1 primary isolates. The cells were cultured without IFN-ε, during which time the supernatants were collected for HIV p24 measurement. The tropisms of the virus isolates are indicated, and viral genotypes are shown in parentheses. (**B**) IFN-ε inhibits single-cycle HIV-luciferase reporter virus. MDMs were treated with IFN-ε (10 ng/ml) for 24 hours and then exposed to pseudotyped HIV-luc (JR-FL). Luciferase activity (RLUs) was normalized to untreated controls. (**C**) HIV inhibition by IFN-ε (10 ng/ml) from different sources. MDMs were pretreated with IFN-ε from yeast, Expi293F cells, and *E. coli* for 24 hours and then infected with HIV-luc (JR-FL). Reduced and alkylated bacteria-expressed IFN-ε was included for comparison. (**D**) Effect of IFN-ε on HIV infection of $CD4^+$ T cells. PHA-activated $CD4^+$ T cells were treated with different amounts of IFN-ε for 24 hours and then infected with HIV-luc (JR-FL) or $HIV\text{-}1_{BaL}$ at different MOIs. IFN-α was included as a comparison. (**E**) Effect of IFN-ε on PMA-differentiated THP-1 cells. PMA-differentiated THP-1 cells were treated with different amounts of IFN-ε or IFN-α for 24 hours and then infected with pseudotyped HIV-luc (VSV-G) in a single-cycle infection assay. (**F**) Effect of IFN-ε on SAMHD1 knockdown THP-1 cells. Cell lines with or without SAMHD1 knockdown were treated with IFN-ε or IFN-α for 24 hours and then infected with pseudotyped HIV-luc (VSV-G). Data in **A**, **E**, and **F** are mean ± SD of triplicate samples and are representative of 3 independent experiments. Actual data points are shown. Dots in **B** (median, IQR), **C** (mean ± SD), and **D** (mean ± SD) represent data from individual donors of 3–12 experiments. *$P < 0.05$, IFN-ε–treated cells vs. untreated controls by independent-samples *t* test.

absence of SAMHD1, whereas IFN-ε exhibited moderate anti-HIV activity in the absence of SAMDH1 (Figure 1F). The degree of HIV inhibition was greater in SAMHD1 knockdown cells compared to THP-1 cells with a control vector (Figure 1F).

Pretreatment with IFN-ε protects macrophages against HIV-1. Pretreatment of MDMs with IFN-ε at 10 ng/ml for 24 hours blocked HIV infection by 70%–98%, depending on donors (Figure 1B and Figure 2A). When MDMs were pretreated with IFN-ε for 2 or 6 hours, the degree of antiviral activity was reduced in MDMs from most donors. In one donor, pretreatment with IFN-ε at 10 ng/ml for 2 hours did not protect cells against HIV infection (donor 2; Figure 2A). IFN-ε at 1 ng/ml for 24 hours blocked HIV infection by 72.5% (average of 3 donors), but the extent of protection varied among different donors. Pretreatment with IFN-ε at 10 ng/ml for 24 hours before HIV infection for 2 hours, followed by adding back IFN-ε at 10 ng/ml, provided nearly complete protection against HIV infection, whereas pretreatment with IFN-ε at 1 ng/ml for 24 hours, followed by adding back IFN-ε at 1 ng/ml provided partial protection (Figure 2B). To determine whether IFN-ε could suppress HIV infection after viral entry, HIV-1–infected MDMs were treated with IFN-ε at 2 hours or 24 hours after virus exposure. IFN-ε at 10 ng/ml blocked HIV infection when infected cells were treated at 2 hours after infection, although the degree of anti-HIV activity was

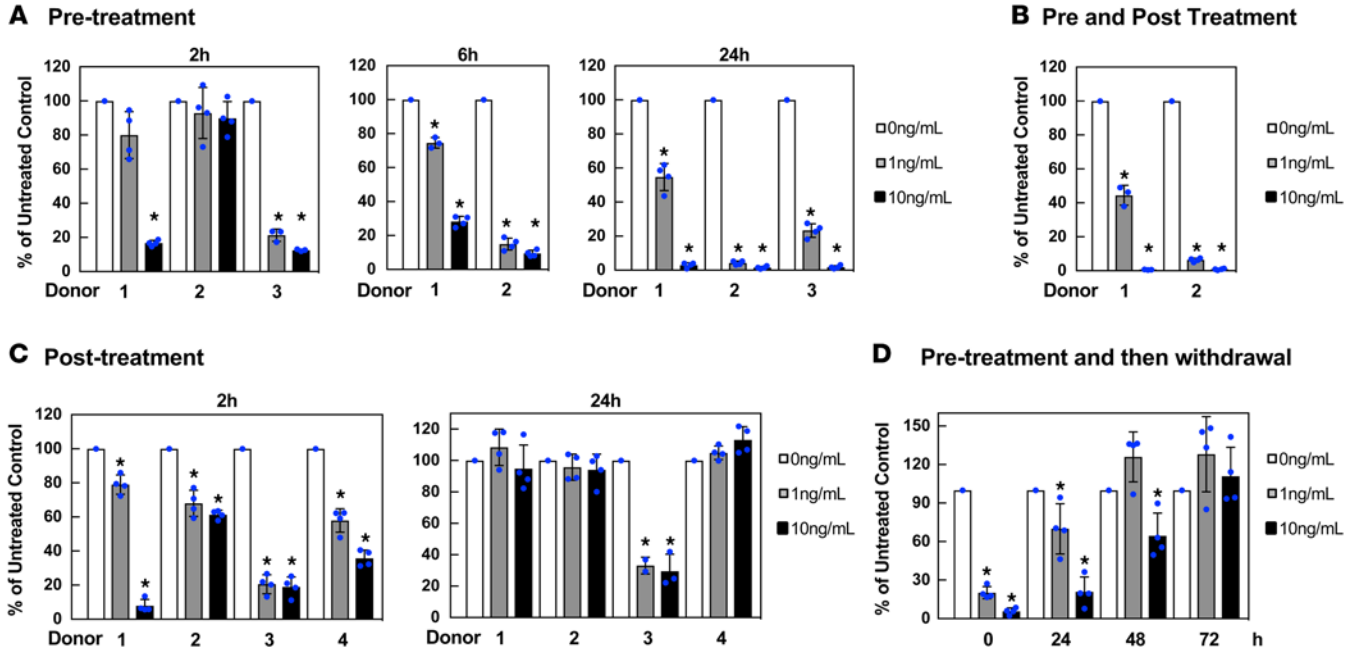

Figure 2. Pretreatment with IFN-ε protects macrophages against HIV-1. (**A**) Effect of pretreatment with IFN-ε on HIV infection. MDMs were treated with IFN-ε for 2, 6, or 24 hours and then infected with HIV. (**B**) Effect before and after treatment with IFN-ε on HIV infection. MDMs were pretreated with IFN-ε for 24 hours and then infected with HIV. IFN-ε (at the pretreatment concentration) was added back during HIV infection. (**C**) Effect of IFN-ε on HIV-infected cells. MDMs were infected with HIV for 2 hours and then treated with IFN-ε immediately or 24 hours after viral infection. (**D**) IFN-ε–mediated HIV protection is reversible. MDMs were treated with IFN-ε for 24 hours, washed, and then cultured in complete medium without IFN-ε for 0, 24, 48, or 72 hours before HIV infection. HIV-luc (JR-FL) was used in all experiments. The absolute value of RLUs in the 0 ng/ml samples ranged from 10^5 to 10^7. Results from different donors are shown in **A**–**C**. The experiment in **D** was repeated in MDMs from another donor. Data are mean ± SD of triplicate samples. *$P < 0.05$, IFN-ε–treated cells vs. untreated controls by independent-samples *t* test.

not as potent as that after pretreatment with HIV-1 for 24 hours (Figure 2C). When cells were treated at 24 hours after HIV exposure, IFN-ε did not block infection of MDMs from 3 of 4 donors, suggesting that IFN-ε blocks early events in HIV infection.

To determine whether the protective effect of IFN-ε was sustained after removal of the cytokine, MDMs were pretreated with IFN-ε for 24 hours, washed with PBS, and then cultured in medium without IFN-ε for 0, 24, 48, or 72 hours before HIV infection. The antiviral activity waned in a time-dependent manner after the removal of IFN-ε and was extinguished by 72 hours (Figure 2D). Taken together, these results indicate that 24-hour treatment is required for maximal anti-HIV activity of IFN-ε and the protective effect is reversible.

IFN-ε pretreatment downregulates CCR5 and blocks reverse transcription and nuclear import. The kinetics of HIV inhibition by IFN-ε (Figure 2) suggested that IFN-ε acted at an early stage of the HIV life cycle. Therefore, we determined whether IFN-ε pretreatment affected receptors required for HIV entry. MDMs from different donors were treated with IFN-ε for 24 hours, and cell surface levels of CD4, CXCR4, and CCR5 were measured by flow cytometry. The results indicated that IFN-ε did not affect CD4 or CXCR4 surface expression but had a significant effect on CCR5 (Figure 3A).

As IFN-ε downregulated CCR5, it would affect the analysis of subsequent steps after viral entry in R5 virus-infected cells in response to IFN-ε. Thus, we determined whether IFN-ε inhibited infection by HIV receptor–independent VSV-G pseudotyped virus. We found that IFN-ε did not affect the attachment of HIV-luc (VSV-G) (Figure 3B) but successfully blocked HIV-luc (VSV-G) infection (Figure 3C), suggesting that IFN-ε also blocked infection after viral entry.

To assess the effect of IFN-ε on HIV reverse transcription, we determined the kinetics of HIV early and late reverse-transcribed (RT) products in MDMs with or without IFN-ε treatment. Results of quantitative real-time PCR analysis showed that the synthesis of both early and late RT products was suppressed in IFN-ε–treated MDMs infected with R5 HIV-1_{BaL} (Figure 3D). However, in MDMs infected with coreceptor-independent HIV-luc (VSV-G), we found that synthesis of late RT but not early RT products was blocked in IFN-ε–treated MDMs (Figure 3E). The reduction of early RT products in R5 virus-infected

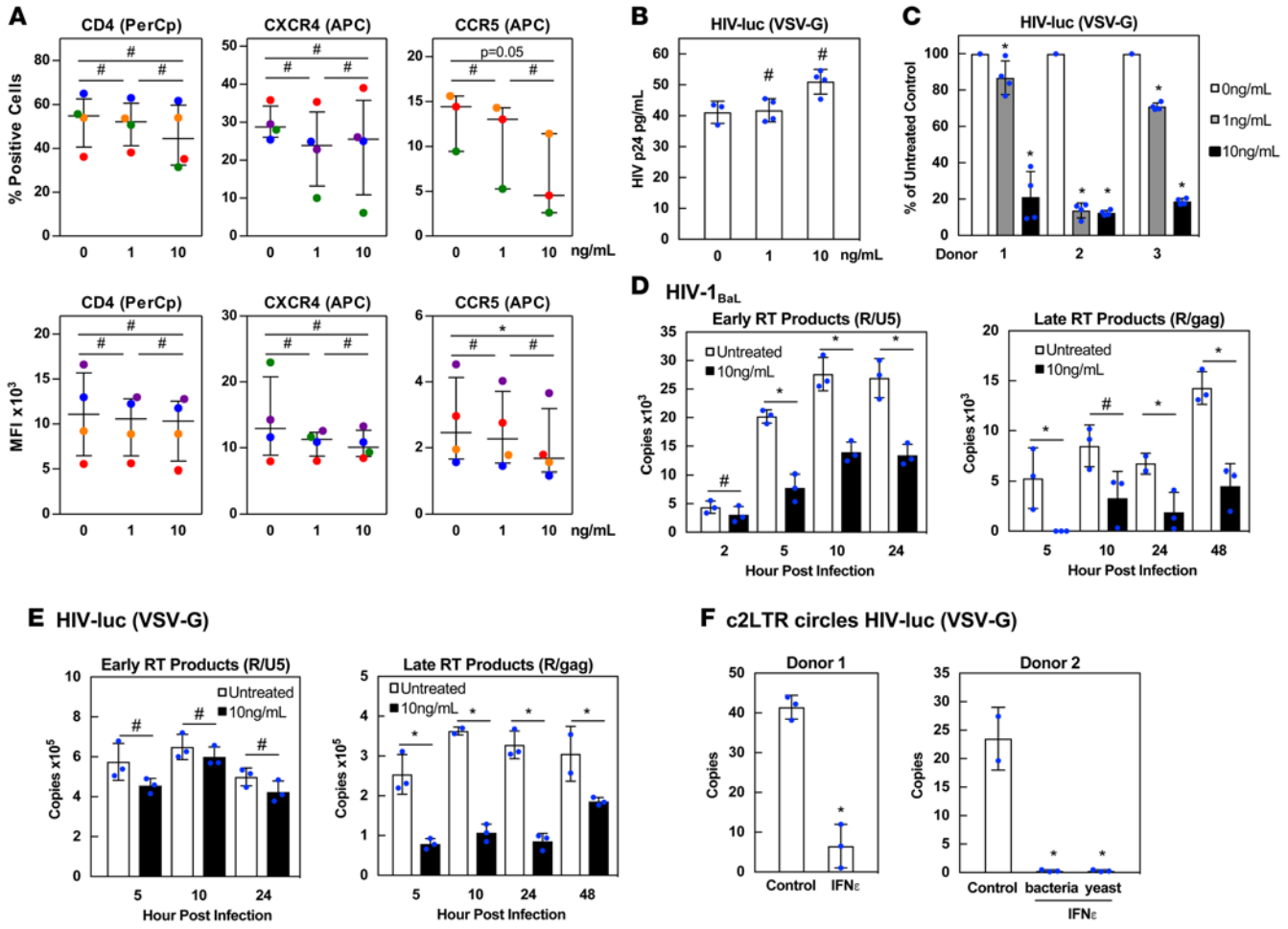

Figure 3. IFN-ε downregulates CCR5 and blocks reverse transcription and nuclear import. (**A**) Effect of IFN-ε on expression of cell surface receptors for HIV entry. MDMs from different donors were treated with IFN-ε for 24 hours, and cell surface expression of CD4, CXCR4, and CCR5 was determined by flow cytometry as percentage of positive cells or MFI. (**B**) Effect of IFN-ε on viral attachment. MDMs were treated with IFN-ε for 24 hours before exposure to HIV-luc (VSV-G) for 2 hours at 4°C. Cells were washed extensively with PBS and then lysed with 1% Triton-X. HIV attachment was determined by measuring cell-associated HIV p24. (**C**) IFN-ε protects MDMs from infection by HIV-luc (VSV-G). MDMs were treated with IFN-ε for 24 hours and then infected with HIV-luc (VSV-G). (**D** and **E**) Effect of IFN-ε on HIV reverse transcription. MDMs were treated with IFN-ε for 24 hours and then infected with HIV-1_{BaL} or HIV-luc (VSV-G). HIV-1 early and late reverse-transcribed (RT) DNA products were measured by quantitative real-time PCR. (**F**) Effect of IFN-ε on HIV nuclear import. MDMs were treated with IFN-ε for 24 hours before infection with HIV-luc (VSV-G). The levels of c2LTR circles at 48 hours after infection were determined by quantitative real-time PCR. $^{*}P < 0.5$, $^{\#}P > 0.05$, IFN-ε treated cells vs. untreated controls by independent-samples *t* test. Dots in **A** (median, IQR) represent data from individual donors. Data in **B**–**E** are mean ± SD of triplicate samples and represent 3 independent experiments using MDMs from different donors.

MDMs may be due to IFN-ε–mediated downregulation of CCR5. To determine whether IFN-ε affected HIV nuclear import, the step after reverse transcription and before integration, we analyzed the level of closed 2-long terminal repeat (c2LTR) circles, a marker of nuclear import, and found significant reduction of c2LTR circles in IFN-ε–treated MDMs from two donors (Figure 3F).

IFN-ε induces type I IFN signaling pathways in primary macrophages. IFN-ε is a type I IFN but only shares 30% homology with IFN-α and IFN-β. The involvement of IFN-ε in the type I IFN signaling pathway has been characterized using bone marrow–derived macrophages from IFN-α receptor knockout mice (*Ifnar1*$^{-/-}$ and *Ifnar2*$^{-/-}$) (21); however, the IFN signaling pathway in response to IFN-ε has not been elucidated in human macrophages. We found that IFN-ε, similar to IFN-α, induced type I IFN-stimulated genes, including *infβ, oas1, mx1, g1p2, and ifit1*, within 6 hours, and expression levels of these genes (except *ifit1*) were further increased at 24 hours (Figure 4A). IFN-ε induced STAT1 phosphorylation (at Tyr701) in multiple cell types, including MDMs, PHA-activated CD4^{+} T cells, and PMA-differentiated SAMHD1 knockdown THP1 cell lines (Figure 4B). In MDMs, the extent of STAT1 phosphorylation

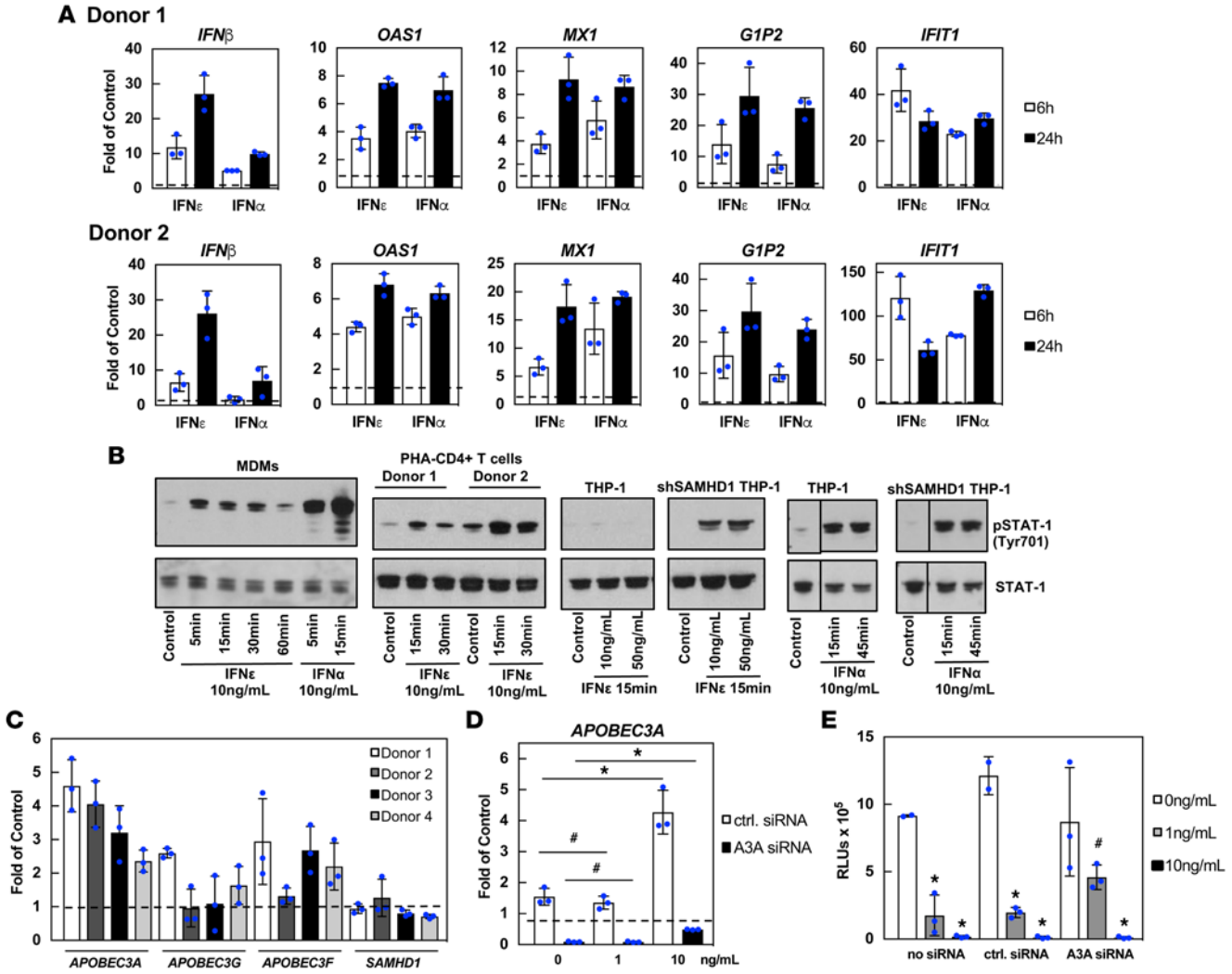

Figure 4. IFN-ε induces type I IFN signaling pathways and host restriction factor APOBEC3A. (**A**) IFN-ε induces type I IFN-stimulated genes (ISGs). MDMs were treated with IFN-ε or IFN-α, and gene expression of ISGs was measured by real-time RT-PCR. Induction of each gene (as fold change relative to control) was calculated using the ΔΔCT method, as described in the Methods. The dashed line indicates the level of gene expression of untreated control cells. (**B**) IFN-ε activates STAT1. STAT1 activation was determined by Western blot using Tyr701 phopho-STAT1 antibody. The blot was stripped and then probed with anti-STAT1 antibody for the loading control. (**C**) Induction of HIV restriction factors by IFN-ε. MDMs were treated with IFN-ε for 24 hours, and the expression of HIV restriction factors was determined by real-time RT-PCR. Each bar represents the fold change between untreated control and IFN-ε–treated MDMs from different donors. The dashed line indicates the level of gene expression of untreated control cells. (**D**) Effect of APOBEC3A knockdown on induction of APOBEC3A by IFN-ε. MDMs were transfected with 10 nM control siRNA or siRNA targeting APOBEC3A (A3A) for 24 hours before incubation with IFN-ε for an additional 24 hours. Expression of A3A was determined by quantitative real-time RT-PCR. $^{*}P < 0.5$, control siRNA vs. A3A siRNA by independent-samples *t* test. (**E**) Effect of IFN-ε on HIV infection of APOBEC3A knockdown MDMs. MDMs were incubated with the transfection reagent alone (no siRNA) or the transfection reagent with control siRNA or A3A siRNA for 24 hours. Cells were then treated with IFN-ε for an additional 24 hours followed by HIV-luc (JR-FL) infection. $^{*}P < 0.05$, $^{\#}P > 0.05$, IFN-ε–treated vs. untreated controls PMA-differentiated PMA-differentiated by independent-samples *t* test. Data are mean ± SD of triplicate samples and represent 3 independent experiments.

induced by IFN-α was much greater than that by IFN-ε (Figure 4B). Finally, IFN-α but not IFN-ε phosphorylated STAT1 in PMA-differentiated THP-1 cells (Figure 4B).

Involvement of HIV host restriction factors in IFN-ε–mediated HIV inhibition. The HIV restriction factors APOBEC3G, APOBEC3F, and SAMHD1 are induced by type I IFNs (37–39). To determine whether IFN-ε induced a host restriction factor(s) in MDMs that led to HIV inhibition, expression of these HIV restriction factors was assessed by real-time RT-PCR in MDMs with or without IFN-ε treatment. As expected, MDMs expressed these HIV host restriction factors (Supplemental Figure 3A). IFN-ε did not induce expression of SAMHD1 (Figure 4C), whereas IFN-α induced SAMHD1 gene expression in 2 of 3 donors (Supplemental Figure 3B). Together with the result in Figure 1F, indicating anti-HIV activity of

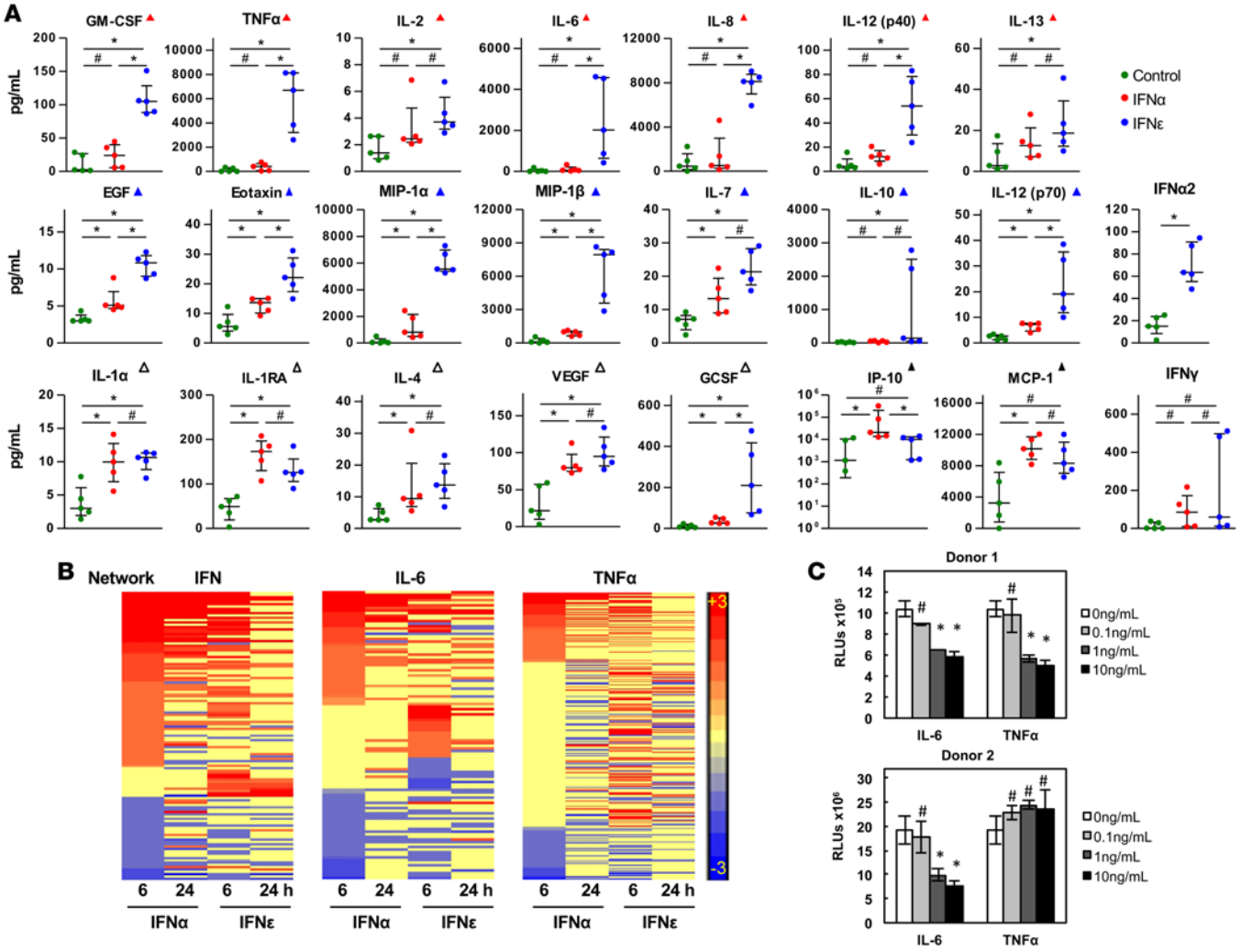

Figure 5. Differential profiles of immune mediators in response to IFN-ε and IFN-α. (**A**) Induction of immune mediators by IFN-ε or IFN-α. MDMs were treated with IFN-ε or IFN-α (both 10 ng/ml) for 6 hours. Levels of cytokines/chemokines in the media were determined by a multiplex assay. Triangles of different colors designate differential regulation between IFN-ε and IFN-α: red triangles denote immune mediators that are induced by IFN-ε but not IFN-α; blue triangles denote immune mediators that are upregulated by IFN-ε to a greater extent than IFN-α; black triangles denote immune mediators that are induced by IFN-α to a greater extent than to IFN-ε; and white triangles denote immune mediators that are similarly responsive to IFN-ε and IFN-α. Mann-Whitney *U* test was used for the statistical analysis. (**B**) Induction of IFN, IL-6, and TNF-α signaling networks by IFN-ε and IFN-α. Intensity maps for expression patterns of genes associated with type I IFN, IL-6, and TNF-α networks in IFN-α– or IFN-ε–stimulated MDMs from 4 donors at 6 or 24 hours. Red color denotes upregulation, blue color denotes downregulation, and yellow color indicates no significant change or absence of expression; color intensity correlates with expression level. The scale bar ranges from +3 (red) to –3 (blue). The complete list of genes in these networks and their expression levels are shown in Supplemental Table 1. (**C**) Effect of IL-6 and TNF-α on HIV infection. MDMs were treated with IL-6 or TNF-α for 24 hours and then infected with HIV-luc (JR-FL). Cytokines were not present during the infection. $^{*}P < 0.05$, $^{\#}P > 0.05$, treated vs. untreated controls by independent-samples *t* test. Dots in **A** represent data from individual donors (median, IQR). Data in **C** are mean ± SD of triplicate samples.

IFN-ε in PMA-differentiated SAMHD1 knockdown THP-1 cells, these results show that SAMHD1 alone is unlikely to play a major role in IFN-ε–mediated HIV inhibition.

IFN-α strongly induced all APOBEC3 genes, particularly APOBEC3A (by 100- to 500-fold) (Supplemental Figure 3B). However, IFN-ε induced some expression, though it was not strong, of these APOBEC3 genes in MDMs from all donors (except APOBEC3G and 3F in donor 2). APOBEC3G and APOBEC3F were moderately induced in 2–3 of 4 donors. However, APOBEC3A was consistently induced to a greater extent among different donors than were APOBEC3G or APOBEC3F (Figure 4C). In light of proposed antiviral activity of APOBEC3A, we tested whether APOBEC3A contributed to IFN-ε–mediated HIV inhibition. Transfection of MDMs with APOBEC3A siRNA knocked down APOBEC3A and blocked the IFN-ε–mediated induction of APOBEC3A (Figure 4D). In APOBEC3A knockdown

MDMs, IFN-ε at 1 ng/ml was less potent in blocking HIV infection, but the concentration of 10 ng/ml remained effective (Figure 4E), suggesting some involvement but not a requirement for APOBEC3A in IFN-ε–mediated HIV inhibition.

MX2 but not MX1 contributes to anti-HIV activity of IFN-α by blocking HIV replication at the step of nuclear import and integration (40). Although IFN-ε induced gene expression of both MX1 and MX2 in MDMs from different donors and MX2 siRNA knockdown slightly increased the degree of HIV infection, MX1 and MX2 siRNA knockdown did not abolish anti-HIV activity of IFN-ε (Supplemental Figure 4).

Differential profiles of immune mediators in response to IFN-ε and IFN-α. To determine whether IFN-ε induced production of a similar set of cytokines/chemokines as IFN-α, MDMs were stimulated with IFN-ε or IFN-α for 6 hours, and soluble immune mediators were determined in the culture medium by multiplex assay (Figure 5A). IFN-ε but not IFN-α significantly induced GM-CSF, TNF-α, IL-2, IL-6, IL-8, IL-12 (p40), and IL-13 (Figure 5A, red triangles). IFN-ε induced more pronounced expression of EGF, eotaxin, MIP-1α, MIP-1β, IL-7, IL-10, and IL-12 (p70) than did IFN-α2 (Figure 5A, blue triangles). IFN-ε and IFN-α induced similar levels of IL-1α, IL-1RA, IL-4, VEFG, and GCSF (Figure 5A, white triangles). IFN-α induced more pronounced expression of IP-10 and MCP-1 than IFN-ε (Figure 5A, black triangles). Induction of IFN-γ by IFN-ε or IFN-α appeared to be donor dependent. IFN-ε also induced low levels of IFN-α in MDMs. Note that MIP-1α and MIP-1β induced by IFN-ε may contribute to downregulation of CCR5 (Figure 3A).

To delineate the signaling pathways regulated by IFN-ε, we determined the global transcriptomes by microarray analysis. IFN-α was included as a comparison. As expected, genes associated with type I IFN signaling were upregulated in MDMs in response to IFN-α or IFN-ε (Figure 5B and Supplemental Table 1). Of the 125 significantly differentially expressed genes (SDEG) in this network, IFN-α upregulated 76 and downregulated 36 genes assessed after 6 hours stimulation; after 24 hours, 51 genes remained upregulated and 26 remained downregulated (Figure 5B). IFN-ε upregulated 59 genes and downregulated 20 genes at 6 hours; after 24 hours, 30 genes remained upregulated and 17 remained downregulated (Figure 5B). Among genes differentially regulated by both IFN-α and IFN-ε at the 6-hour time point, all except TAP1, UBQLN1, EIF3c, and BCL10 were regulated in the same direction (up or down). IFN-ε upregulated a subset of genes at the 6-hour time point that were not regulated by IFN-α at 6 hours; these included TNFRSF4, IFNL1, CD40, IL18RAP, REL, BCL3, HEXB, IL18, STAT4, and IL1B. Expression of the majority genes induced by IFN-ε had returned to basal levels at the 24-hour time point (Figure 5B).

Because IFN-ε induced expression of IL-6 and TNF-α (Figure 5A), we assessed expression of genes associated with these cytokine networks. Of the 111 SDEG in the IL-6 network, at the 6-hour time point IFN-ε regulated expression of 74 genes (41 upregulated and 33 downregulated), whereas IFN-α regulated the expression of 79 genes (44 upregulated; 35 downregulated). At the 24-hour time point, the numbers of genes upregulated or downregulated by IFN-α or IFN-ε were reduced by 30% (Figure 5B and Supplemental Table 1). IFN-ε uniquely regulated a subset of cytokines/chemokine genes, including IL-6, CCL1, MMP10, IL-19, IL-36RN, TNFSF9, and IL27-RA (Supplemental Table 1).

With respect to the TNF-α network, at the 6-hour time point, IFN-ε regulated more genes than IFN-α: IFN-ε regulated 142 genes (104 upregulated and 38 downregulated), whereas IFN-α regulated 116 genes (66 upregulated and 50 downregulated) (Figure 5B and Supplemental Table 1). Of possible importance, IFN-ε but not IFN-α upregulated expression of genes coding for proinflammatory molecules, including TNF-α, IL-23A, IL-12B, CXCL1, CXCL2, CXCL3, IL-1A, IL-2RA, CCL19, MMP1, HIF1, and SOD2. At the 24-hour time point, the numbers of genes regulated by either IFN-ε or IFN-α were significantly reduced. Of relevance to the role of IFN-ε in HIV infection, IL-6 exhibited anti-HIV activity in MDMs from two different donors and TNF-α exhibited activity in one of the donors (Figure 5C), indicating that both cytokines have some effects in some donors and that induction of IL-6 or TNF-α does not entirely contribute to anti-HIV activity of IFN-ε.

IFN-ε induces ROS that protects macrophages against infection. Immune activation has been shown to enhance phagocytosis and induce production of ROS, which play an important role in control of infection (41–47). Transcriptome analysis indicated that IFN-ε but not IFN-α induced the expression of genes involved in phagocytosis and ROS production (Figure 6A). Among the 54 SDEG associated with phagocytosis, at the 6-hour time point, IFN-α upregulated 14 genes and IFN-ε upregulated 37 genes. The number of downregulated genes was comparable between the two groups (IFN-α downregulated 14 genes and IFN-ε downregulated 17 genes) (Figure 6A and Supplemental Table 2). IFN-ε upregulated genes encoding

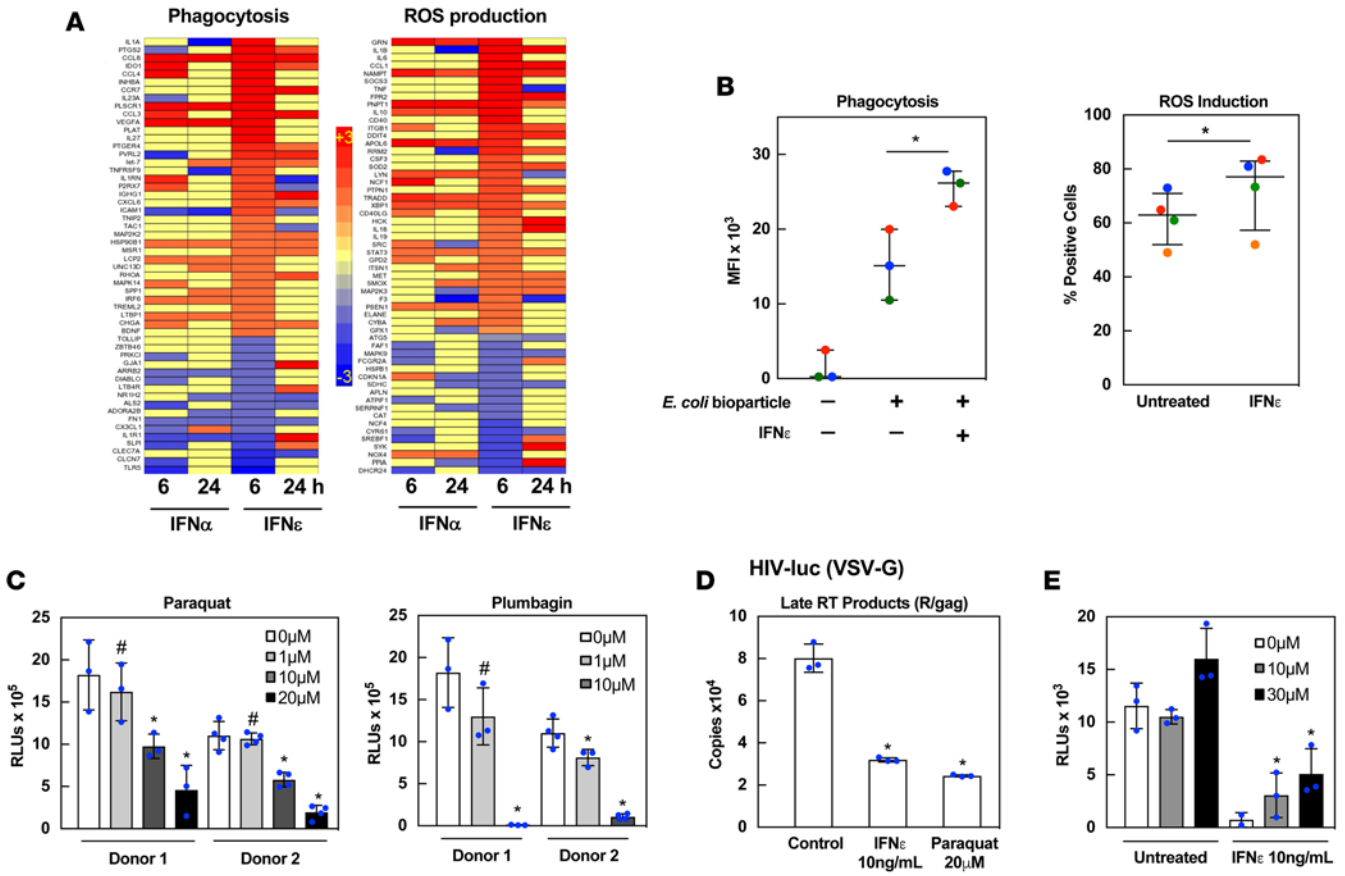

Figure 6. IFN-ε induces ROS that protects macrophages against HIV infection. (**A**) Effect of IFN-α and IFN-ε on genes involved in phagocytosis and ROS production. Intensity maps for expression pattern of genes associated with phagocytosis and ROS generation networks in MDMs in response to IFN-α or IFN-ε for 6 or 24 hours. Red color denotes upregulation, blue color denotes downregulation, and yellow color denotes no significant change or absence of expression; color intensity correlates with expression level. The scale bar ranges from +3 (red) to –3 (blue). The complete list of genes in these networks and their expression levels are shown in Supplemental Table 2. (**B**) Effect of IFN-ε on phagocytosis and ROS induction. IFN-ε–treated or untreated MDMs were incubated with Texas Red fluorescent *E. coli* BioParticles, and phagocytic activity was determined by flow cytometry. MDMs with or without IFN-ε treatment for 24 hours were stained with carboxy-H2DCFDA, and the ROS level was determined by flow cytometry. The gate for percentage of positive cells was based on unstained control cells. Results (median, IQR) from different donors are shown. (**C**) Effect of ROS induction on HIV infection. MDMs were treated with ROS inducers paraquat or plumbagin for 24 hours before infection with HIV-luc (JR-FL). ROS inducers were not added back during infection. $^{*}P < 0.05$, $^{\#}P > 0.05$, untreated controls vs. treated MDMs. (**D**) Effect of a ROS inducer on HIV late RT synthesis. MDMs were treated with paraquat or IFN-ε for 24 hours and infected with HIV-luc (VSV-G). The levels of HIV RT DNA products were determined at 24 hours after infection by quantitative real-time PCR. $^{*}P < 0.05$, treated vs. untreated control. (**E**) Effect of ROS inhibition on IFN-ε–mediated HIV inhibition. MDMs were treated with or without IFN-ε for 4 hours and were then treated with NAC in the presence of IFN-ε for 2 hours before infection with HIV-luc (JR-FL). IFN-ε and NAC were not added back during the infection. $^{*}P < 0.05$ IFN-ε–treated MDMs in the presence or absence of NAC. Data in **C**–**E** are mean ± SD of triplicate samples. Results in **D** and **E** represent 3 independent experiments by by independent-samples *t* test.

cell membrane receptors involved in phagocytosis, including TNFRSF9, MSR1, PTGER4, and CCR7. At the 24-hour time point, among IFN-α–induced, phagocytosis-related genes, 11 remained upregulated, and among IFN-ε–induced genes, 19 remained upregulated. Similar numbers of SDEG (8 genes) were downregulated in response to either stimulus.

Analysis of 56 SDEG associated with ROS generation indicated that 68% (38 genes) were upregulated by IFN-ε and about 30% (17 genes) were upregulated by IFN-α after 6 hours stimulation (Figure 6A and Supplemental Table 2). Nearly 50% of genes in this pathway were not significantly affected by IFN-α. IFN-ε upregulated genes that code for cellular enzymes associated with ROS production, including CYBA, ELANE, GPX1, PTPN1, RRM2, SDHC, and SOD2. At the 24-hour time point, among IFN-ε–induced genes, 21 remained upregulated, and among IFN-α–induced genes, 14 remained upregulated.

Consistent with the transcriptome results, the ability of IFN-ε to induce phagocytosis and ROS production was also shown by flow cytometry (Figure 6B). ROS play an important role in modulating innate immunity (48). To determine the effect of ROS on HIV inhibition, MDMs were treated with noncytotoxic concen-

trations of the ROS inducers paraquat or plumbagin (Supplemental Figure 5). Both paraquat and plumbagin blocked HIV infection of MDMs (Figure 6C), suggesting a negative effect of ROS on HIV infection. Similar to IFN-ε, paraquat reduced the levels of late RT products (Figure 6D), indicating that ROS induction inhibited reverse transcription. To assess the role of ROS in IFN-ε–mediated HIV inhibition, an ROS scavenger, N-acetyl-L-cysteine (NAC), was used. In agreement with previous reports using replication-competent viruses (49, 50), we found that short-term treatment with NAC at high concentration (10 mM) blocked single-cycle HIV infection, but NAC at concentrations of 100 μM or lower did not exhibit anti-HIV activity (Supplemental Figure 6). We found that NAC at low concentrations (10–30 μM) diminished IFN-ε–mediated HIV inhibition in a dose-dependent manner (Figure 6E). The incomplete block of IFN-ε–mediated HIV inhibition may be a consequence of pleiotropic effects of NAC on HIV and immune functions.

Discussion

IFN-ε is expressed in the female genital tract (21), and its levels are modulated by estrogen (21), TNF-α (30), and seminal plasma (31), suggesting a role in HIV transmission. We found that IFN-ε protected primary macrophages but not transformed cell lines. It had little or no effect in primary activated $CD4^+$ T cells, unless a low MOI was used. IFN-ε pretreatment for 2 hours was sufficient to protect MDMs against HIV in 2 of 3 donors. Treatment for 24 hours was required to achieve the maximal protective effect, suggesting that the anti-HIV activity induced by IFN-ε requires activation of cellular response such as ROS induction. IFN-ε pretreatment also suppressed HIV infection in 3 of 4 donors when added 2 hours after viral exposure but was not effective when infected cells were treated 24 hours after infection. IFN-ε pretreatment downregulated CCR5 in all donors, but downregulation of CD4 and CXCR4 was donor dependent. Taken together, our results indicate that IFN-ε protects macrophages from HIV infection by induction of CC-chemokines, downregulation of CCR5, and inhibition of reverse transcription and nuclear import.

Distinct functions between IFN-ε and other type I IFNs, such as IFN-α/β, have been documented in other systems, although not in primary macrophages. For example, IFN-ε is constitutively expressed in mucosal epithelium, whereas expression of IFN-α/β is low but is induced in response to pattern recognition receptor activation (21). The in vitro antiviral activity of IFN-ε against VSV-infected WISH cells is relatively weak compared with IFN-α (26). In our study, IFN-α exhibited more potent anti-HIV activity than IFN-ε, completely blocking HIV infection in PMA-differentiated THP-1 cells at 10 ng/ml, at which concentration IFN-ε had no effect. In SAMHD knockdown cell lines, which exhibit hyper IFN responsiveness (51, 52), treatment with IFN-α at 10 ng/ml completely suppressed HIV infection, whereas IFN-ε at 10 or 50 ng/ml blocked HIV infection by 48% or 68%, respectively. Interestingly, IFN-ε induced STAT1 phosphorylation in SAMHD knockdown cells but not THP-1 cells, despite weak signals. The signal of STAT1 phosphorylation was stronger in THP-1 or SAMHD1 knockdown cells in response to IFN-α than IFN-ε. Coincidentally, the degree of STAT1 phosphorylation appeared to associated with anti-HIV activity of IFNs in THP-1 cell lines. The role of STAT1 activation in IFN-ε–mediated HIV inhibition remains to be determined. With respect to anti-HIV activity, IFN-ε exhibited a similar cellular preference as IFN-α, both exhibiting more pronounced effects in MDMs than $CD4^+$ T cells (53–55).

In addition to exhibiting different levels of anti-HIV activity, IFN-α and IFN-ε induced partially overlapping sets of cytokines/chemokines and signaling pathways. In comparison with IFN-α, IFN-ε significantly induced higher levels of cytokines and chemokines that modulate HIV transmission (10, 56, 57), suggesting an important role in innate immune regulation at the mucosa. The immune-modulatory function of IFN-ε has been investigated with respect to NK cell function. IFN-ε potently promotes NK cell cytotoxicity (26), which may play a role in protection against chlamydial infection of the female genital tract (58). Similarly, IFN-ε induced more robust phagocytosis and ROS production in 6 hours than IFN-α, suggesting a role in the initial innate immune response. It is possible that IFN-ε is involved in the first line of immune surveillance.

Differential induction of immune mediators by IFN-α and IFN-ε was also supported by transcriptome analysis. We found that the numbers of genes induced or the levels of induction of type I IFN, IL-6, and TNF pathways in response to IFN-α and IFN-ε were not identical, despite some overlap. Analysis of selected networks showed that IFN-α regulated more genes and more upregulated genes than IFN-ε in the type I IFN signaling network; whereas IFN-ε regulated more genes in the TNF-α pathway, phagocyte activation, and ROS generation. Although both IFNs induced genes associated with IL-6 pathways, the repertoires of genes were different. There was an early immune activation (6

hour) in both IFN-α and IFN-ε–stimulated MDMs that waned by 24 hours. Many of the molecular correlates of this immune activation were sustained to a greater extent by IFN-α than IFN-ε at 24 hours. Despite conservation of core gene sets and conservation of their expression patterns between IFN-α and IFN-ε stimulation, unique sets of genes associated with immune activation networks were differentially regulated by these two cytokines. The distinct kinetics of immune pathways and gene sets suggest that IFN-α and IFN-ε participate in specific, distinct immune response pathways in addition to their overlapping, compensatory immune functions.

Consistent with previous findings on HIV restriction of SAMHD1 (51, 59), the degree of HIV infection was significantly higher in PMA-differentiated, SAMHD1 knockdown THP1 cells than cells with SAMHD1. SAMHD1 gene expression was not induced by IFN-ε in primary macrophages. IFN-ε exhibited anti-HIV activity in SAMHD1 knockdown THP-1 macrophages, suggesting that SAMHD1 is not required for IFN-ε–mediated HIV inhibition. Another HIV host restriction factor regulated by IFN-α, APOBEC3A, has been shown to block the early phase of HIV infection of myeloid cells, including macrophages (39, 60). Although we did not observe an increase in HIV infection in APOBEC3A knockdown MDMs, as in a previous report (39), suppression of APOBEC3A expression led to a partial reversal of HIV inhibition by low-concentration IFN-ε, suggesting the involvement of APOBEC3A in anti-HIV activity of IFN-ε. APOBEC3A knockdown had no effect on HIV inhibition by higher concentrations of IFN-ε, suggesting that multiple host factors, rather than APOBEC3A alone, contributed to IFN-ε–mediated HIV inhibition. IFN-inducible antiviral factor MX2 is known to block the step of nuclear import and integration during HIV infection (40). Both IFN-ε and IFN-α induced MX1 and MX2 (Supplemental Figure 4A). Although we observed a slight increase in HIV infection in MX2 knockdown MDMs (Supplemental Figure 4B). MX2 siRNA did not effect the anti-HIV activity of IFN-ε (Supplemental Figure 4B), suggesting that MX2 alone does not contribute to IFN-ε–mediated HIV inhibition.

One possible mechanism by which IFN-ε protected MDMs against HIV was by increasing phagocytic activities and ROS production. Genes involved in phagocytosis and ROS production were strongly induced in response to IFN-ε. Additionally, IFN-ε increased ROS production in MDMs, which suppressed HIV infection and blocked HIV late RT synthesis. The mechanism of ROS-mediated inhibition of HIV RT synthesis requires further thorough investigation. ROS may reduce RT products by sheering nucleic acids via the hydroxyl radical (61) or by blocking enzymes or metabolites through oxidation (41, 62). Induction of ROS by IFN-ε leads to oxidization of reverse transcriptase, which would reduce the enzyme's processivity, affecting synthesis of late RT products more than the early RT products, as seen in HIV-luc (VSV-G)infected MDMs with IFN-ε treatment.

NAC at 5–20 mM has been shown to block HIV infection, particularly at the step of transcription (49, 50, 63, 64). Lower concentrations of NAC (10–30 μM) did not have an effect on HIV infection but reduced IFN-ε–mediated HIV inhibition. NAC suppressed production of TNF-α but not of IL-6 or IL-1α in LPS-treated mice (65). It is possible that IFN-ε induces multiple cytokines that stimulate ROS production, and perhaps NAC can only block the actions of some of these cytokines, which may explain the partial reversal of IFN-ε–mediated HIV inhibition. Additionally, regulation of ROS levels can be complex depending on specific ROS species, the sources of ROS, free amino acids, and expression of genes associated with redox signaling pathways in response to IFN-ε and cytokines induced by IFN-ε.

The role of IFN-ε in HIV transmission and pathogenesis in vivo has not been defined. Frequent semen exposure in HIV-negative sex workers is associated with an increase in IFN-ε gene expression in the cervical epithelium (32). In contrast to IFN-α induced by viral infection, IFN-ε expression is not altered in the gut mucosa of rhesus macaques in response to SIV infection (24). Both blocking IFN-I receptor function and administration of IFN-α2 result in greater $CD4^+$ T cell depletion and faster disease progression in SIV-infected macaques (11). It remains to be determined whether functions of IFN-ε distinct from IFN-α contribute to this paradoxical result. Since IFN-ε expression can be regulated by hormones and proinflammatory cytokines such as TNF-α, further investigation of the association between IFN-ε and parameters important for HIV susceptibility, immune activation, and disease progression will offer a better understanding of the function of type I IFNs in HIV infection.

In summary, we describe the anti-HIV activity of IFN-ε and its mechanism in primary macrophages. We also present several immune functions of IFN-ε distinct from IFN-α. In concert with its properties at the mucosa, our findings indicate that IFN-ε may play a role in HIV transmission and immune-related diseases.

Methods

Reagents. Histopaque-1077, FBS, human serum AB, RPMI-1640, DMEM, PBS, PHA, PMA, PmB, NAC, and lipopolysaccharides from *E. coli* 055:B5 (LPS) were from Sigma-Aldrich. Human IFN-α2a was purchased from PBL Assay Science. Human IL-2, IL-6, and TNF-α were from R&D Systems. PerCP-conjugated mouse IgG1κ anti-human CD4 antibody (clone RPA-T4), PerCP mouse IgG1κ isotype control antibody, and APC mouse IgG_{2a} κ isotype control antibody were from BioLegend. APC-conjugated mouse IgG_{2a} κ anti-human CD184 antibody (CXCR4, clone 12G5) and APC-conjugated mouse IgG_{2a} κ anti-human CD195 (CCR5, clone 3A9) were from BD Biosciences. Recombinant human IFN-ε expressed in yeast (*Pichia Pastoris*) was custom-made by MyBioSource and was further purified using Pierce High-Capacity Endotoxin Removal Spin Columns (Thermo Fisher Scientific). The endotoxin level in the IFN-ε stock was below 0.01 ng/ml, as determined by using the Pierce LAL Chromogenic Endotoxin Quantitation Kit (Thermo Fisher Scientific). The identity of IFN-ε was confirmed by Western blot and mass spectrometry.

Expression of recombinant IFN-ε from E. coli and human cell lines. The DNA constructs to express recombinant human IFN-ε in *E. coli* and in human cells were synthesized and verified by Genescript. For bacterial expression, a codon-optimized IFN-ε cDNA was cloned into pET28. Inclusion bodies of IFN-ε expressed in *E. coli* BL21 were dissolved in 8 M GuHCl in the presence of DTT, purified by reversed-phase HPLC, and lyophilized. For oxidative folding, reduced IFN-ε was dissolved at 0.2 mg/ml in 8 M GuHCl, followed by an 8-fold dilution with 50 mM Tris/HCl buffer containing 3 mM reduced glutathione and 0.3 mM oxidized glutathione, pH 8.3. After 1.5 hours, the folding solution was purified on a Waters XBridge C4 column, and folded IFN-ε protein with one disulfide bond formed was verified by electrospray ionization mass spectrometry. To prepare linear alkylated IFN-ε, reduced IFN-ε was dissolved at 1 mg/ml in 8 M GuHCl, followed by an 8-fold dilution with 50 mM Tris/HCl buffer containing the nonthiol-reducing agent TCEP and Cys-reactive iodoacetamide (the weight ratio of IFN-ε, TCEP, and iodoacetamide = 1:1:1), and, after 30 minutes, HPLC purification to homogeneity was performed. Mass spectrometric analysis indicated addition of 3 iodoacetamide molecules to the 3 Cys residues of IFN-ε.

The construct used to express IFN-ε proteins in cell lines was modified by replacing the native signal peptide (MIIKHFFGTVLVLLASTTIFS) with an artificial signal peptide (MGWSCIILFLVATAGVHS) to overcome the reported block of secretion by fibroblasts and cell lines (25). Constructs in pcDNA3 vector with a C-terminal His Tag were generated. For expression, an Expi293 Expression System Kit (Life Technologies) was used according to the manufacturer's instructions. IFN-ε proteins in supernatants were obtained at day 3 after transfection and enriched using Ni-NTA beads (Qiagen). Imidazole-eluted proteins were concentrated and washed using an Amicon Ultra-15 Centrifugal Filter Unit with a 10-KDa cutoff (EMD Millipore). IFN-ε proteins were verified by Western blot analysis with anti-IFN-ε (Atlas) and anti-His tag antibodies. IFN-ε from yeast was used in most experiments and verified using proteins from other sources. The yeast version was used because the large quantities available allowed us to repeat experiments in MDMs from various donors.

Cell isolation and culture. PBMCs were isolated from the blood of healthy human donors obtained from the New York Blood Center by Histopaque-1077 gradient centrifugation. MDMs were prepared as described previously (66). $CD4^+$ T cells were negatively selected from PBMCs by depletion of magnetically labeled non-$CD4^+$ T cells using the $CD4^+$ T cell Isolation Kit II from Miltenyi Biotec. Purified $CD4^+$ T cells were activated with PHA (5 μg/ml) and IL-2 (50 IU/ml) for 3 days in RPMI-1640 with 10% FBS. Activated cells were washed with PBS and cultured in the presence of IL-2. THP-1 cell lines were differentiated in RPMI containing PMA (33 ng/ml) for 24 hours before use. THP-1 cell lines were from ATCC and were maintained in the Chang and Landau's laboratories. THP-1 SAMHD knockdown cell lines were generated by Nathaniel Landau at New York University School of Medicine. HEK-293T and HeLa-CD4-CCR5 cells (provided by David Kabat at Oregon Health & Science University, Portland, Oregon) were maintained in DMEM with 10% FBS.

HIV-1 infection. Replication-defective pseudotyped luciferase-expressing reporter viruses, HIV-luc (JR-FL) or HIV-luc (VSV-G), used in single-cycle infection assays were produced in HEK293T cells by cotransfection of a plasmid encoding the envelope-deficient HIV NL4-3 virus and luciferase reporter gene (pNL-Luc-R+E-) along with a plasmid encoding $HIV\text{-}1_{JR\text{-}FL}$ Env gp160 or VSV-G as described previously (67, 68).

Replication-competent HIV-1 T/F viruses were generated through Lipofectamine 2000 transfection of HEK-293T cells with a plasmid containing the full-length HIV-1 virus (plasmids obtained from John

Kappes, NIH AIDS Reagent Program, Division of AIDS, National Institute of Allergy and Infectious Diseases [NIAID], Panel of Infectious Molecular Clones [catalog 11919]). Viruses were propagated in PHA-activated PBMCs. HIV-1_{BaL} virus was from Advanced Biotechnologies Inc. HIV-1 primary isolates were obtained from the UNAIDS Network for HIV Isolation and Characterization (Division of AIDS, NIAID) and were propagated in PHA-activated $CD4^+$ T cells.

For single-cycle infection assays, $CD4^+$ T cells at 1×10^6 per sample or MDMs at 7×10^4 per sample were infected with pseudotyped luciferase reporter viruses (~10 ng HIV p24 per sample) for 2 hours at 37°C. After washing off unbound virus, cells were cultured for 3 days before lysis in passive lysis buffer (Promega). Luciferase activity (in RLUs) was measured on a 2300 EnSpire Multilabel Plate Reader (PerkinElmer). To summarize the results from multiple donors, the average percentage of control was calculated using the following formula: (RLUs of treated cells/RLUs of untreated cells) × 100.

For multiple-round infection assays, cells were exposed to replication-competent viruses at a MOI of 0.05 for 2 hours at 37°C. After washing off unbound virus, cells were cultured, and HIV-1 p24 levels in cell culture supernatant were measured at different time points after viral infection by the AlphaLISA HIV p24 kit (PerkinElmer).

To determine the effect of IFN-ε on HIV attachment, MDMs were treated with IFN-ε for 24 hours before exposure to HIV-luc (VSV-G) for 1.5 hours at 4°C, washed 6 times with PBS, and then lysed with 1% Triton-X before measuring cell-associated HIV p24.

Cytotoxicity assay. MDMs were plated in 96-well plates at 25,000 cells per well and then treated with various concentrations of IFN-ε for 24 hours. After 24 hours, IFN-ε was removed, and cells were cultured for an additional 3 days. Cell viability was analyzed using the CytoTox-Glo Cyotoxicity assay (Promega), and the percentage of viable cells was calculated using the following formula: percentage viable cells = (total luminescence – dead cell luminescence)/total luminescence × 100.

Flow cytometry. To determine cell surface expression of CD4 and HIV coreceptors, MDMs were collected by incubation at 4°C in PBS for 30 minutes using cell scrapers. Cells were blocked in wash buffer (PBS, 2% FBS, 1% human serum AB) on ice for 20 minutes and then stained with fluorochrome-conjugated specific antibodies against CD4, CXCR4, or CCR5 and with appropriate isotype controls in wash buffer for 20 minutes. Cells were washed, fixed with 2% paraformaldehyde in PBS, and analyzed using a BD Accuri C6 flow cytometer (BD Biosciences). Results were analyzed with FlowJo (Tree Star Inc.).

To determine the level of ROS, MDMs with or without treatment were incubated in 10 μM carboxy-H2DCFDA (Life Technologies) in PBS for 40 minutes at 37°C. Cells were washed once and immediately analyzed by flow cytometry. The phagocytosis assay was performed by incubating MDMs with Texas Red fluorescent *E. coli* BioParticles (Molecular Probes) for 30 minutes at 37°C. Cells were washed, fixed, and analyzed by flow cytometry.

Real-time RT-PCR. Total RNA was isolated using TRIzol (Life Technologies). First-strand cDNA was synthesized by incubating 1,000 ng total RNA with oligo$(dT)_{12–18}$ (25 μg/ml) and dNTP (0.5 mM) at 65°C for 5 minutes followed by quick chilling on ice. Reverse transcription was performed at 42°C for 50 minutes and 70°C for 15 minutes using SuperScript III Reverse Transcriptase. The PCR reaction contained cDNA equivalent to 30 ng of RNA input, 200 nM of primer sets, and SYBR Green Master Mix (QIAGEN) and was run in a StepOnePlus real-time PCR system (Life Technologies). PCR conditions included 95°C denaturation for 10 minutes, 40 cycles of 95°C for 15 seconds, and 60°C for 60 seconds. PCR products were quantified and normalized relative to the amount of GAPDH cDNA products. Relative quantification of gene expression was calculated using the ΔΔCt (Ct, threshold cycle of real-time PCR) method according to the following formulas: $\Delta CT = Ct_{GAPDH\ rRNA} - Ct_{target}$, $\Delta\Delta Ct = \Delta Ct_{control} - \Delta Ct_{IFN\text{-}\varepsilon}$, ratio $= 2^{-\Delta\Delta Ct}$. Primer sequences were as follows: GAPDH forward (5′-TGAAGGTCGGAGTCAACGGATTTGG-3′), GAPDH reverse (5′-CATGTGGGCCATGAGGTCCACCAC-3′); APOBEC3A forward (5′-TGGCATTGGAAGGCATAAGAC-3′), APOBEC3A reverse (5′-TTAGCCTGGTTGTGTAGAAAGC-3′); APOBEC3F forward (5′-TACGCAAAGCCTATGGTCGG-3′), APOBEC3F reverse (5′-GCTCCAAGATGTGTACCAGG-3′); APOBEC3G forward (5′-GGCTCCACATAAACACGGTTTC-3′), APOBEC3G reverse (5′-AAGGGAATCACGTCCAGGAA-3′); SAMHD1 forward (5′-CCAAGCGTCCCCGTTGCGAT-3′), and SAMHD1 reverse (5′-TCAAAGCCACCGCGCCTGAG-3′). The IFNr qRT-primer set (InvivoGen) was used to characterize IFN-induced genes in MDMs treated with IFN-α or IFN-ε.

Quantitative PCR analysis of HIV-1 DNA. Total DNA was purified from HIV-1_{BaL}- or HIV-luc (VSV-G)–infected MDMs using the QIAamp DNA Blood Mini Kit (Qiagen). The levels of HIV DNA

products were quantified by real-time PCR using total DNA (100 ng or 200–300 ng for RT DNA products or c2LTR circles, respectively), 200 nM primers, and SYBR Green Master Mix. The primer sequences for HIV-1 early RT products were M667 (5′-GGCTAACTAGGGAACCCACTG-3′) and AA55 (5′-CTGCTAGAGATTTTCCACACTGAC-3′); the primers for HIV-1 late RT products were M667 (shown above) and M661 (5′-CCTGCCTCGAGAGAGCTCCACACTGAC-3′) (69). The primer sequences for HIV-1 c2-LTR circles were 515 (5′-GTGTGTAGTTCTGCTAATCAGGGAA-3′) and 9600 (5′-GCTTAAGCCTCAATAAAGCTTGCCT-3′) (70). Standard curves for early or late RT products were generated with 10-fold serial dilutions of pNL4-3.Luc.R-E- ranging from 10^1 to 10^8 copies. Standard curve for c2-LTR circles was generated with 10-fold serial dilutions of pTA2LTR plasmid ranging from 10^1 to 10^5 copies. PCR cycling conditions were 95°C for 10 minutes, followed by 40 cycles of 95°C for 15 seconds and 60°C for 60 seconds.

Multiplex cytokine/chemokine assay. Cytokines and chemokines in conditioned media from MDMs with or without IFN treatment were analyzed using a MAGPIX multiplexing instrument (EMD Millipore) and a Milliplex Map human cytokine/chemokine magnetic bead panel kit (EMD Millipore, catalog HCYTMAG-60K-PX29) according to the manufacturer's instructions. Results were analyzed using Millipore Analyst software.

Western blot. One million cells were lysed on ice for 10 minutes in cell lysis buffer (Cell Signaling) containing 1× Halt Protease inhibitor (Thermo Scientific), 1 mM PMSF, and 10 mM sodium fluoride. Proteins were resolved in NuPAGE Novex 4%–12% Bis-Tris Protein Gels (Life Technologies) followed by Western blot analysis using pY701 STAT-1 antibody (BD Biosciences) or STAT-1 antibody (Cell Signaling) at a 1:1,000 dilution overnight at 4°C. Peroxidase-labeled anti-mouse or anti-rabbit antibody (KPL) at a 1:10,000 dilution was used for detection with the Amersham ECL Western Blotting Detection Kit.

siRNA. MDMs were incubated with Viromer Blue transfection reagent (Lipocalyx) alone or in the presence of 10 nM AllStars negative control siRNA (Qiagen) or Hs_APOBEC3A_1 FlexiTube siRNA (Qiagen) for 24 hours. Following transfection, cells were treated with IFN-ε for 24 hours and then exposed to HIV-luc (JR-FL) for 2 hours. HIV infection was determined by measuring luciferase activity at day 3 after infection.

Microarray analysis. Gene expression profiling was performed using the Affymetrix GeneChip Human Gene 1.0 ST Array (Affymetrix Inc.). Total RNA was isolated using the miRNeasy Mini Kit (Qiagen) and was converted to cDNA following the GeneChip WT Plus Reagent Kit protocol. Briefly, total RNA (300 ng) was used for first- and second-strand cDNA synthesis. cRNA was obtained by an in vitro transcription reaction and was then used as the template for generating first-strand cDNA. The cDNA was fragmented and end-labeled with biotin. The biotin-labeled cDNA was hybridized to the array for 16 hours at 45°C using the GeneChip Hybridization Oven 640. Washing and staining with streptavidin-phycoerythrin was performed using the GeneChip Hybridization, Wash, and Stain Kit, and the GeneChip Fluidics Station 450. Images were acquired using the GeneChip Scanner 3000 7G and the GeneChip Command Console Software. Normalized and background-corrected, raw probe intensity values were uploaded to Partek Genomics Suite version 6.5 (PARTEK Inc.) for further analysis as described previously (71). Briefly, the $\log_2$-transformed expression intensity data from IFN-treated samples ($n = 4$ per group per time point) were compared with the pooled data from the untreated samples ($n = 4$). One-way ANOVA was applied to determine differentially expressed genes in IFN-treated samples relative to the untreated samples at 6 or 24 hours after treatment. A false discovery rate of 5% was set as the cutoff to SDEG. Microarray data have been submitted to GEO (accession GSE83716).

Pathway/network analysis. To identify the pathways/networks and biological functions perturbed in MDMs, the list of SDEG from MDMs treated with IFN for 6 or 24 hours, relative to the untreated MDMs, was analyzed using Ingenuity Pathway Analysis (INGENUITY, Qiagen) as described previously (71). Fisher's exact test was used to calculate P values used to rank networks of SDEG. $P < 0.05$ was considered statistically significant.

Statistics. Statistical comparisons were performed using 2-tailed independent-samples t test or Mann Whitney U test as indicated. IBM SPSS Statistics (version 22) was used. $P < 0.05$ was considered significant.

Study approval. The buffy coat was purchased from the New York Blood Center. Purchased blood samples were exempt from approval because they were distributed without identifiers. The Institutional Review Board approval for the use of human blood was obtained from Rutgers New Jersey Medical School.

Author contributions

CT, PG, JC, and CL performed HIV infection, IFN-ε preparation, and gene expression experiments. SS, SG, and PS performed microarray and data analysis. SS, PS, XZ, NL, and WL were involved in experimental designs, data discussion, and manuscript preparation. TLC oversaw the entire project, designed experiments, and prepared the manuscript. All authors read and approved the final manuscript.

Acknowledgments

We thank Pam De Lacy and her team at Shenandoah Biotechnology Inc. for production of IFN-ε proteins in *E. coli*, William Honnen for his technical assistant on production of IFN-ε proteins in Expi293F cells, Jaeha Kim for the technical support, and the Center for Advanced Proteomics Research for the mass spectrometry analysis. We also thank Fred Biollet-Ruche, Joan E. Durbin, and Patricia Fitzgerald-Bocarsly for helpful discussions. This work was supported by NIH grants R01AI081559 and R01AI110372 to TLC. The mass spectrometry data were obtained from a Orbitrap instrument funded in part by NIH grant NS046593 for the support of the Neuroproteomics Core Facility at Rutgers New Jersey Medical School.

Address correspondence to: Theresa L. Chang, Public Health Research Institute, Rutgers New Jersey Medical School, 225 Warren Street, Newark, New Jersey 07103, USA. Phone: 973.854.3265; E-mail: Theresa.chang@rutgers.edu.

1. Trinchieri G. Type I interferon: friend or foe? *J Exp Med*. 2010;207(10):2053–2063.
2. Pestka S. Purification and cloning of interferon alpha. *Curr Top Microbiol Immunol*. 2007;316:23–37.
3. Kawai T, Akira S. The role of pattern-recognition receptors in innate immunity: update on Toll-like receptors. *Nat Immunol*. 2010;11(5):373–384.
4. González-Navajas JM, Lee J, David M, Raz E. Immunomodulatory functions of type I interferons. *Nat Rev Immunol*. 2012;12(2):125–135.
5. Schoggins JW, et al. A diverse range of gene products are effectors of the type I interferon antiviral response. *Nature*. 2011;472(7344):481–485.
6. McNab F, Mayer-Barber K, Sher A, Wack A, O'Garra A. Type I interferons in infectious disease. *Nat Rev Immunol*. 2015;15(2):87–103.
7. Cho H, Kelsall BL. The role of type I interferons in intestinal infection, homeostasis, and inflammation. *Immunol Rev*. 2014;260(1):145–167.
8. Teijaro JR, et al. Persistent LCMV infection is controlled by blockade of type I interferon signaling. *Science*. 2013;340(6129):207–211.
9. Ng CT, et al. Blockade of interferon Beta, but not interferon alpha, signaling controls persistent viral infection. *Cell Host Microbe*. 2015;17(5):653–661.
10. Katsikis PD, Mueller YM, Villinger F. The cytokine network of acute HIV infection: a promising target for vaccines and therapy to reduce viral set-point? *PLoS Pathog*. 2011;7(8):e1002055.
11. Sandler NG, et al. Type I interferon responses in rhesus macaques prevent SIV infection and slow disease progression. *Nature*. 2014;511(7511):601–605.
12. Hughes R, Towers G, Noursadeghi M. Innate immune interferon responses to human immunodeficiency virus-1 infection. *Rev Med Virol*. 2012;22(4):257–266.
13. Oldstone MB. A Jekyll and Hyde profile: type 1 interferon signaling plays a prominent role in the initiation and maintenance of a persistent virus infection. *J Infect Dis*. 2015;212 Suppl 1:S31–S36.
14. Zuniga EI, Hahm B, Oldstone MB. Type I interferon during viral infections: multiple triggers for a multifunctional mediator. *Curr Top Microbiol Immunol*. 2007;316:337–357.
15. Doyle T, Goujon C, Malim MH. HIV-1 and interferons: who's interfering with whom? *Nat Rev Microbiol*. 2015;13(7):403–413.
16. Poli G, Biswas P, Fauci AS. Interferons in the pathogenesis and treatment of human immunodeficiency virus infection. *Antiviral Res*. 1994;24(2-3):221–233.
17. Schnittman SM, Vogel S, Baseler M, Lane HC, Davey RT. A phase I study of interferon-alpha 2b in combination with interleukin-2 in patients with human immunodeficiency virus infection. *J Infect Dis*. 1994;169(5):981–989.
18. Sedaghat AR, et al. Chronic CD4+ T-cell activation and depletion in human immunodeficiency virus type 1 infection: type I interferon-mediated disruption of T-cell dynamics. *J Virol*. 2008;82(4):1870–1883.
19. Sivaraman V, Zhang L, Su L. Type I interferon contributes to CD4+ T cell depletion induced by infection with HIV-1 in the human thymus. *J Virol*. 2011;85(17):9243–9246.
20. Sivro A, Su RC, Plummer FA, Ball TB. Interferon responses in HIV infection: from protection to disease. *AIDS Rev*. 2014;16(1):43–51.
21. Fung KY, et al. Interferon-ε protects the female reproductive tract from viral and bacterial infection. *Science*. 2013;339(6123):1088–1092.
22. Hardy MP, Owczarek CM, Jermiin LS, Ejdebäck M, Hertzog PJ. Characterization of the type I interferon locus and identification of novel genes. *Genomics*. 2004;84(2):331–345.
23. Xi Y, Day SL, Jackson RJ, Ranasinghe C. Role of novel type I interferon epsilon in viral infection and mucosal immunity. *Mucosal Immunol*. 2012;5(6):610–622.

24. Demers A, et al. The mucosal expression pattern of interferon-ε in rhesus macaques. *J Leukoc Biol*. 2014;96(6):1101–1107.
25. Hermant P, Francius C, Clotman F, Michiels T. IFN-ε is constitutively expressed by cells of the reproductive tract and is inefficiently secreted by fibroblasts and cell lines. *PLoS One*. 2013;8(8):e71320.
26. Peng FW, et al. Purification of recombinant human interferon-epsilon and oligonucleotide microarray analysis of interferon-epsilon-regulated genes. *Protein Expr Purif*. 2007;53(2):356–362.
27. Day SL, Ramshaw IA, Ramsay AJ, Ranasinghe C. Differential effects of the type I interferons alpha4, beta, and epsilon on antiviral activity and vaccine efficacy. *J Immunol*. 2008;180(11):7158–7166.
28. Cho HR, Kim SK, Lim HK, Jeong Park H, Chung JH, Lee MH. Association study between nonsense polymorphism (rs2039381, Gln71Stop) of interferon-ε and susceptibility to vitiligo in Korean population. *Immunol Invest*. 2013;42(5):423–430.
29. Kim SK, et al. T Allele of nonsense polymorphism (rs2039381, Gln71Stop) of interferon-ε is a risk factor for the development of intracerebral hemorrhage. *Hum Immunol*. 2014;75(1):88–90.
30. Matsumiya T, Prescott SM, Stafforini DM. IFN-epsilon mediates TNF-alpha-induced STAT1 phosphorylation and induction of retinoic acid-inducible gene-I in human cervical cancer cells. *J Immunol*. 2007;179(7):4542–4549.
31. Sharkey DJ, Macpherson AM, Tremellen KP, Robertson SA. Seminal plasma differentially regulates inflammatory cytokine gene expression in human cervical and vaginal epithelial cells. *Mol Hum Reprod*. 2007;13(7):491–501.
32. Abdulhaqq SA, et al. HIV-1-negative female sex workers sustain high cervical IFNε, low immune activation, and low expression of HIV-1-required host genes. *Mucosal Immunol*. 2016;9(4):1027–1038.
33. Keele BF, et al. Identification and characterization of transmitted and early founder virus envelopes in primary HIV-1 infection. *Proc Natl Acad Sci USA*. 2008;105(21):7552–7557.
34. Goujon C, et al. Evidence for IFNα-induced, SAMHD1-independent inhibitors of early HIV-1 infection. *Retrovirology*. 2013;10:23.
35. Dragin L, et al. Interferon block to HIV-1 transduction in macrophages despite SAMHD1 degradation and high deoxynucleoside triphosphates supply. *Retrovirology*. 2013;10:30.
36. Gramberg T, et al. Restriction of diverse retroviruses by SAMHD1. *Retrovirology*. 2013;10:26.
37. Hrecka K, et al. Vpx relieves inhibition of HIV-1 infection of macrophages mediated by the SAMHD1 protein. *Nature*. 2011;474(7353):658–661.
38. Goila-Gaur R, Strebel K. HIV-1 Vif, APOBEC, and intrinsic immunity. *Retrovirology*. 2008;5:51.
39. Berger G, et al. APOBEC3A is a specific inhibitor of the early phases of HIV-1 infection in myeloid cells. *PLoS Pathog*. 2011;7(9):e1002221.
40. Goujon C, et al. Human MX2 is an interferon-induced post-entry inhibitor of HIV-1 infection. *Nature*. 2013;502(7472):559–562.
41. Nathan C, Cunningham-Bussel A. Beyond oxidative stress: an immunologist's guide to reactive oxygen species. *Nat Rev Immunol*. 2013;13(5):349–361.
42. Schroder K, Hertzog PJ, Ravasi T, Hume DA. Interferon-gamma: an overview of signals, mechanisms and functions. *J Leukoc Biol*. 2004;75(2):163–189.
43. Marchi LF, Sesti-Costa R, Ignacchiti MD, Chedraoui-Silva S, Mantovani B. In vitro activation of mouse neutrophils by recombinant human interferon-gamma: increased phagocytosis and release of reactive oxygen species and pro-inflammatory cytokines. *Int Immunopharmacol*. 2014;18(2):228–235.
44. West AP, et al. TLR signalling augments macrophage bactericidal activity through mitochondrial ROS. *Nature*. 2011;472(7344):476–480.
45. West AP, Shadel GS, Ghosh S. Mitochondria in innate immune responses. *Nat Rev Immunol*. 2011;11(6):389–402.
46. Dupré-Crochet S, Erard M, Nüβe O. ROS production in phagocytes: why, when, and where? *J Leukoc Biol*. 2013;94(4):657–670.
47. Dröge W. Free radicals in the physiological control of cell function. *Physiol Rev*. 2002;82(1):47–95.
48. Kohchi C, Inagawa H, Nishizawa T, Soma G. ROS and innate immunity. *Anticancer Res*. 2009;29(3):817–821.
49. Ho WZ, Douglas SD. Glutathione and N-acetylcysteine suppression of human immunodeficiency virus replication in human monocyte/macrophages in vitro. *AIDS Res Hum Retroviruses*. 1992;8(7):1249–1253.
50. Lioy J, Ho WZ, Cutilli JR, Polin RA, Douglas SD. Thiol suppression of human immunodeficiency virus type 1 replication in primary cord blood monocyte-derived macrophages in vitro. *J Clin Invest*. 1993;91(2):495–498.
51. Behrendt R, et al. Mouse SAMHD1 has antiretroviral activity and suppresses a spontaneous cell-intrinsic antiviral response. *Cell Rep*. 2013;4(4):689–696.
52. Zhang R, Bloch N, Nguyen LA, Kim B, Landau NR. SAMHD1 restricts HIV-1 replication and regulates interferon production in mouse myeloid cells. *PLoS One*. 2014;9(2):e89558.
53. Baca-Regen L, Heinzinger N, Stevenson M, Gendelman HE. Alpha interferon-induced antiretroviral activities: restriction of viral nucleic acid synthesis and progeny virion production in human immunodeficiency virus type 1-infected monocytes. *J Virol*. 1994;68(11):7559–7565.
54. Cheney KM, McKnight Á. Interferon-alpha mediates restriction of human immunodeficiency virus type-1 replication in primary human macrophages at an early stage of replication. *PLoS One*. 2010;5(10):e13521.
55. Goujon C, Malim MH. Characterization of the alpha interferon-induced postentry block to HIV-1 infection in primary human macrophages and T cells. *J Virol*. 2010;84(18):9254–9266.
56. Introini A, Vanpouille C, Lisco A, Grivel JC, Margolis L. Interleukin-7 facilitates HIV-1 transmission to cervico-vaginal tissue ex vivo. *PLoS Pathog*. 2013;9(2):e1003148.
57. Kedzierska K, Crowe SM. Cytokines and HIV-1: interactions and clinical implications. *Antivir Chem Chemother*. 2001;12(3):133–150.
58. Hansbro PM, et al. Role of NK cells in IFN-epsilon-mediated protection against female reproductive tract infection (MUC2P.925). *J Immunol*. 2015:194 (Supplement 1); 65.8.
59. Laguette N, et al. SAMHD1 is the dendritic- and myeloid-cell-specific HIV-1 restriction factor counteracted by Vpx. *Nature*. 2011;474(7353):654–657.
60. Peng G, et al. Myeloid differentiation and susceptibility to HIV-1 are linked to APOBEC3 expression. *Blood*. 2007;110(1):393–400.
61. Chiou SH. DNA- and protein-scission activities of ascorbate in the presence of copper ion and a copper-peptide complex. *J Biochem*. 1983;94(4):1259–1267.

62. Pinti M, et al. The role of mitochondria in HIV infection and its treatment. *J Exp Clin Med*. 2010;2(4):145–155.
63. Kalebic T, Kinter A, Poli G, Anderson ME, Meister A, Fauci AS. Suppression of human immunodeficiency virus expression in chronically infected monocytic cells by glutathione, glutathione ester, and N-acetylcysteine. *Proc Natl Acad Sci U S A*. 1991;88(3):986–990.
64. Roederer M, Staal FJ, Raju PA, Ela SW, Herzenberg LA, Herzenberg LA. Cytokine-stimulated human immunodeficiency virus replication is inhibited by N-acetyl-L-cysteine. *Proc Natl Acad Sci U S A*. 1990;87(12):4884–4888.
65. Peristeris P, et al. N-acetylcysteine and glutathione as inhibitors of tumor necrosis factor production. *Cell Immunol*. 1992;140(2):390–399.
66. Tasker C, Ding J, Schmolke M, Rivera-Medina A, García-Sastre A, Chang TL. 17β-estradiol protects primary macrophages against HIV infection through induction of interferon-alpha. *Viral Immunol*. 2014;27(4):140–150.
67. Connor RI, Sheridan KE, Ceradini D, Choe S, Landau NR. Change in coreceptor use correlates with disease progression in HIV-1--infected individuals. *J Exp Med*. 1997;185(4):621–628.
68. Chang TL, Vargas J, DelPortillo A, Klotman ME. Dual role of alpha-defensin-1 in anti-HIV-1 innate immunity. *J Clin Invest*. 2005;115(3):765–773.
69. Zack JA, Arrigo SJ, Weitsman SR, Go AS, Haislip A, Chen IS. HIV-1 entry into quiescent primary lymphocytes: molecular analysis reveals a labile, latent viral structure. *Cell*. 1990;61(2):213–222.
70. Cara A, et al. Circular viral DNA and anomalous junction sequence in PBMC of HIV-infected individuals with no detectable plasma HIV RNA. *Virology*. 2002;292(1):1–5.
71. Subbian S, et al. Early innate immunity determines outcome of Mycobacterium tuberculosis pulmonary infection in rabbits. *Cell Commun Signal*. 2013;11:60.